

Journal of Materials Chemistry B

Accepted Manuscript



This is an *Accepted Manuscript*, which has been through the Royal Society of Chemistry peer review process and has been accepted for publication.

Accepted Manuscripts are published online shortly after acceptance, before technical editing, formatting and proof reading. Using this free service, authors can make their results available to the community, in citable form, before we publish the edited article. We will replace this *Accepted Manuscript* with the edited and formatted *Advance Article* as soon as it is available.

You can find more information about *Accepted Manuscripts* in the [Information for Authors](#).

Please note that technical editing may introduce minor changes to the text and/or graphics, which may alter content. The journal's standard [Terms & Conditions](#) and the [Ethical guidelines](#) still apply. In no event shall the Royal Society of Chemistry be held responsible for any errors or omissions in this *Accepted Manuscript* or any consequences arising from the use of any information it contains.

1 **Water-soluble inclusion complex of fullerene with γ -cyclodextrin**
2 **polymer for photodynamic therapy**

3 Wang Zhang,^{abc} Xiangdong Gong,^a Chang Liu,^d Yuanzhe Piao,^{*bc} Yun Sun^{*d} and
4 Guowang Diao^{*a}

6 **Abstract**

7 A stable aqueous inclusion complex of fullerene (C60) with macromolecules
8 (C60 concentration as high as 3×10^{-4} mol·L⁻¹) was achieved by a one-step strategy
9 using γ -cyclodextrin polymer (γ -CDP). The inclusion complex of C60 with γ -CDP
10 (C60- γ -CDP) was characterized by ultraviolet-visible, Raman, ¹H-NMR
11 spectroscopies, powder X-ray diffraction analysis, and thermogravimetric analysis.
12 The supramolecular interaction and the equilibrium constant for a 1:2 (C60:CD unit in
13 γ -CDP) complex of C60 with γ -CDP were studied. Under ultraviolet A (UVA)
14 irradiation C60- γ -CDP in water could generate singlet oxygen, which was detected by
15 electron paramagnetic resonance spectra. We also evaluated the cytotoxicities of
16 C60- γ -CDP, and investigated the phototoxicity of C60- γ -CDP and pristine C60
17 toward B16-F10 melanoma cells. The cell viability test showed that C60- γ -CDP had
18 significantly higher photodynamic ability than that of the pristine C60 under UVA

^a College of Chemistry and Chemical Engineering, Yangzhou University, Yangzhou, 225002 Jiangsu, P. R. China. E-mail: gw_diao@yzu.edu.cn; Tel: +86 51487975436, Fax: +86 514 87975244

^b Graduate School of Convergence Science and Technology, Seoul National University, Seoul, 151-742, Republic of Korea. E-mail: parkat9@snu.ac.kr; Tel: +82 318889141

^c Advanced Institutes of Convergence Technology, Suwon, 443-270, Republic of Korea.

^d College of Medicine, Yangzhou University, Yangzhou, 225002 Jiangsu, P. R. China. E-mail: ysun@yzu.edu.cn; Tel: +86 51487341733

19 irradiation. This work demonstrated both a CDP-functionalized strategy for enhancing
20 the water-solubility and phototoxicity of fullerenes for applications to cancer
21 photodynamic therapy, as well as a remediation for the negative biological effects of
22 pristine fullerenes.

23

24 **1. Introduction**

25 Cyclodextrins (CDs) are commercially available cyclic oligosaccharides,
26 constituted of 6, 7 or 8 glucose units linked by α -1,4-glucosidic bonds.¹ The most
27 commonly used CD has an internal cavity diameter varying among 5, 7 and 9 Å for α -,
28 β - or γ -CD, respectively. Given the hydrophobic internal cavity and hydrophilic
29 external surface of CDs,² CDs have frequently been applied in many fields, such as
30 electrochemistry,^{3, 4} biotechnology,⁵⁻⁷ and environmental protection,^{8, 9} because their
31 enchanting molecular structures can form supramolecular host-guest complexes with
32 various hydrophobic molecules. CD Polymer (CDP) with the complex forming
33 properties of CD and high solubility, so it can either partially or entirely accommodate
34 suitably sized hydrophobic molecules^{10, 11} or nanomaterials,¹² and form the
35 water-soluble host-guest inclusion complexes with hydrophobic and van der Waals
36 interactions. Moreover, it has gained increasing attention and been widely exploited
37 for biomedical science in the recent years.¹³⁻¹⁵

38 Currently, various applications of Fullerenes (C60s) have been rapidly increased
39 in wide industrial fields and biomedicines due to their unique electronic properties
40 and biological activities.¹⁶ Specifically, C60, as a carbonaceous nanomaterial, can be

41 photo-chemically activated under photo-irradiation to produce singlet oxygen ($^1\text{O}_2$)
42 with high quantum efficiency.¹⁷⁻¹⁹ The process can make effective sensitized oxidation
43 of organic pollutants and inactivation of cells with relatively low energy input.²⁰
44 However, the potential application of fullerene as a biochemical photocatalyst in
45 water treatment is limited owing to the hydrophobic surface of C60. In spite of these
46 unique photochemical, electrochemical, and mechanical properties of C60, its
47 extremely poor water-solubility has significantly impeded medicinal applications.²¹⁻²³
48 Therefore, the method to disperse C60 in water has been one of the hot topics for the
49 past few years. Similarly, much effort has been focused on the increase of C60
50 water-solubility by designing several water-soluble fullerene derivatives
51 approaches.²⁴⁻²⁶ However, the chemical modifications usually restrict C60
52 photo-physical properties.^{27, 28} Therefore, solubilization of C60 with non-covalent
53 approaches is good for photochemical applications of C60. CD, as a suitable
54 solubilizing agent, can provide hydrophobic cavities in aqueous solutions for C60 to
55 form inclusion complexes because of their suited cavity size.²⁹ Furthermore, the
56 formation of C60 inclusion complexes with CD can significantly reduce C60
57 aggregation, preserving the photosensitizing ability of C60.

58 In a previous study, we reported the formation of stable inclusion complex of
59 C60 with β -CDP (C60- β -CDP).¹² As we known, C60-CD complexes were widely
60 used in biomedical applications,³⁰ and there was no report about the degradation of
61 CD in the presence of $^1\text{O}_2$. Because the reactions of $^1\text{O}_2$ often involved carbon-carbon
62 double bond, such as Alder-ene reaction, and Diels-Alder reaction.³¹ However, CD in

63 water did not have the chemical structure which could react with $^1\text{O}_2$. It was meant
64 that C60-CD complexes could be stable when the generation of $^1\text{O}_2$, which provided
65 advantageous conditions for its aqueous application. Here, γ -CDP was chosen as the
66 host polymer because of its high water-solubility and right cavity size for C60. The
67 supramolecular interaction between γ -CDP and C60 was firstly discussed. We also
68 evaluated the ability of C60 inclusion complex with γ -CDP (C60- γ -CDP) to generate
69 $^1\text{O}_2$ after ultraviolet A (UVA) irradiation, and determined the excellent photodynamic
70 activity of C60- γ -CDP against cancer cells. The result reserved that
71 CDP-functionalized methodology of fullerenes without any chemical modification
72 was advantageous to investigate the structure–performance relationship between
73 fullerenes with supramolecular chemistry to design compounds for special
74 applications.

75

76 **2. Experimental**

77 **2.1. Reagents**

78 Fullerene (C60), γ -cyclodextrin (γ -CD), epichlorohydrin (EP), ethylene glycol,
79 and 2,2,6,6-tetramethyl-4-piperidone (TEMP) were purchased was purchased from
80 Sigma-Aldrich. Double distilled and sterilized water was used to prepare all solution.

81 RPMI 1640 medium and fetal bovine serum were purchased from Thermo
82 Scientific. 3-(4,5-dimethylthiazol-2-yl)-2,5-diphenyltertazolium bromide (MTT) was
83 purchased from Sigma Chemical Co. Penicillin and streptomycin were from Beyotime
84 Institute of Biotechnology.

85

86 2.2. Apparatus

87 The molecular-weight distribution of γ -CD polymer was determined by gel
88 permeation chromatography (GPC) Agilent 1100 series (Agilent, USA) with
89 PLaquagel-OH MIXED 8 μm column. Ultraviolet-visible (UV) spectra were recorded
90 on the UV spectrum photometer (Shimadzu, UV-2550) equipped with a quartz cell (1.0
91 cm optical path length). The ^1H NMR spectra were conducted on a 600 MHz NMR
92 spectrometer (Bruker, AVANCE 600) at 303.1 K in deuterium oxide. The powder
93 X-ray diffraction spectra (XRD) were measured by a X-ray instrument (Bruker, D8
94 super speed) with Cu $K\alpha$ radiation, $\lambda=1.542 \text{ \AA}$. The Raman measurements were
95 carried out on a Raman system (Renishaw, Renishaw inVia). Thermo gravimetric
96 analysis (TGA) was performed on a thermogravimetric analyzer (PerkinElmer, Pyris 1
97 TGA) with 10 mg samples which was heated from room temperature to 700 $^\circ\text{C}$ at a
98 rate of 10 $^\circ\text{C}\cdot\text{min}^{-1}$ under nitrogen atmosphere. Electron Paramagnetic Resonance
99 (EPR) Spectra were carried out with a EPR spectrometer (Bruker., A300-10/12) under
100 the following conditions: 10 mW microwave power, 100 kHz modulation frequency, 1
101 G modulation amplitude, scan time 8 min, and 80 G scan range. The microscopic
102 observation of the preliminary cell viability assay was used by a light microscopy
103 (Nikon, 80i). The optical density of each well was measured at 570 nm using a
104 microplate reader (Bio-TEK, elx800).

105

106 2.3. Preparation of γ -CD polymer and C60- γ -CD polymer inclusion complex

107 The water-soluble γ -CDP was obtained by polymerization of γ -CD with EP
108 under a strongly alkaline condition (30 wt% NaOH), which were close to the ones
109 described the methods of preparation of water-soluble CD polymer.^{10, 32, 33}

110 The synthesis and purification of C60- γ -CDP were shown as follow: it was
111 prepared by dissolving 4 g γ -CDP and 2 g C60 in 100 ml water with sufficiently
112 stirring for at least 48 h at room temperature. At the end of the reaction, a brown
113 solution contained C60- γ -CDP was obtained after filtrating to remove insoluble C60.
114 After that, 200 ml ethanol was added into the solution. The inclusion complex
115 precipitated from the solution. Then C60- γ -CDP was isolated by filtration using a
116 membrane filter (pore size: 0.3 μ m), and washed by ethanol. The inclusion complex
117 was dried in a vacuum oven at 60 °C for 24 h. The schematic illustration of γ -CDP,
118 C60, and C60- γ -CDP was shown in Fig. 1.

119

120 **2.4. Singlet Oxygen Detection by Electron Paramagnetic Resonance**

121 Singlet oxygen was detected by an EPR method using TEMP as a spin-trapping
122 reagent. To 5 mL C60- γ -CDP and TEMP aqueous solution (C60 in C60- γ -CDP: 80
123 μ M, TEMP: 40 mM) was introduced into a flat cell, irradiated with a 300 W
124 photo-reflector lamp at a distance of 10 cm, and immediately subjected to EPR
125 measurement. The generation of $^1\text{O}_2$ was detected as an EPR signal due to TEMPO
126 formed by the reaction of $^1\text{O}_2$ with TEMP.¹⁸ Radiation from the lamp was passed
127 through a glass filter to remove wavelengths below 300 nm.

128

129 **2.5. Cell culture**

130 The mouse melanoma cell lines B16–F10 were purchased from the Cell Bank of the
131 Chinese Academic of Sciences. The mouse melanoma B16–F10 was maintained at
132 37 °C at 5% CO₂ in RPMI 1640 medium supplemented with 10% fetal bovine serum,
133 penicillin and streptomycin.

134

135 **2.6. Cell Viability**

136 The photocytotoxicity test was described in the previous study with minor
137 modifications.^{34,35} Briefly, B16–F10 cells were plated at a density of 4×10^5 cells ml⁻¹
138 in 96-well plates in RPMI 1640 medium supplemented with 10% fetal bovine serum
139 for 1 h. After that, the medium was removed and replaced by sterile PBS. The cells
140 were cultured in dark for 2 h at 37 °C to different C60- γ -CDP in phosphate buffer
141 solution (PBS). Also, control cells were treated with PBS alone. Cells were then
142 irradiated with UVA from two fluorescent PUVA lamps (Philips, PL-L36W) or two
143 cool white visible light lamps (Philips, TLD36W). After 20 minutes of exposure, the
144 PBS solution was removed and replaced with cell culture medium, and the cells were
145 kept in the incubator overnight. 20 μ l of MTT (5 mg·ml⁻¹) was added to each well, and
146 the cells were further incubated for an additional 4 h. After incubation, media was
147 removed and DMSO was added to dissolve purple precipitates. Then plates were read
148 at 570 nm using a microplate reader (Bio Tek, EXL800).

149

150 **2.7. Statistical analysis**

151 Statistical analyses were conducted using SPSS ver 11.5. Results are expressed
152 as mean \pm SEM. and the significance of differences was determined using the
153 two-way analysis of variance (ANOVA) followed by Student-Newman-Keuls multiple
154 comparison test (SNK) as post hoc. Differences were consider significant if $P < 0.05$.

155

156 **3. Results and discussion**

157 **3.1. Aqueous solubility and dissociated constant of C60- γ -CDP**

158 C60 is essentially insoluble in water. It was observed that C60 (10 mg) did not
159 dissolve in water (10 mL) even upon stirring at 25 °C for 24 h, as shown in Fig. 2A
160 (a). However, C60 suspension was obtained when 100 mg of CDP was used and
161 stirred at 25 °C for 24 h by a magnetic stirrer. The suspension was centrifuged in
162 order to separate the undissolved C60 precipitates. After filtration, a brown filtrate
163 was obtained in Fig. 2A (b). This result showed γ -CDP as the solubilizing agent made
164 C60 dispersing in water, indicating that γ -CDP, as well as γ -CD³⁶ and β -CD
165 polymer,¹² could form inclusion complexes with C60.

166 Fig. 2B shows the UV absorption spectra of C60 (a) and C60- γ -CDP (b) in water.
167 Because of the poor water-solubility of C60, no absorption of C60 was observed in
168 the range of 200-800 nm as shown in Fig. 2B (a). However, the UV spectrum of
169 C60- γ -CDP showed a characteristic absorption band at 220, 272, and 333 nm
170 corresponding to the chromophoric C60 molecules in Fig. 2B (b), thereby proving that
171 the C60 molecules were dissolved in water and γ -CDP served as the solubilizing agent.
172 Compared with the UV spectrum of C60- γ -CD in water,³⁷ the three absorption bands

173 in Fig. 2B (b) red-shifted, indicating that C60s could form inclusion complexes with
174 γ -CDP.

175 Fig. 3A shows the UV spectra of C60- γ -CDP with different concentrations in
176 aqueous solution. The peak positions were independent of the concentrations of
177 C60- γ -CDP, suggested that C60 could not form C60 aggregation in water with γ -CDP.
178 It was meant that the supramolecular interaction prevented C60 from forming the
179 aggregation in water. Moreover, the peaks intensity increased with the concentration
180 of C60- γ -CDP. Plotting the absorbance of C60- γ -CDP at 272 nm versus the
181 concentration of C60- γ -CDP, a straight line was obtained as shown in Fig. 3B.
182 According to the Lambert-Beer law, the absorption coefficient (ϵ) of C60- γ -CDP in
183 aqueous solution (pH=7.0, 25°C) were evaluated as 1.31 L·g⁻¹·cm⁻¹.

184 In order to study the supramolecular interaction between C60 and γ -CDP, the
185 Benesi-Hildebrand method was used by the UV spectrum.³⁸ Because of the
186 insolubility of C60 in water, ethylene glycol, as a suitable solvent for C60 and γ -CDP,
187 was chosen to study the dissociated constant of the inclusion complex. The formation
188 of C60- γ -CDP in ethylene glycol could be confirmed by the UV spectrum as shown in
189 Fig. 4A, where the concentration of CD unit in γ -CDP was varied from 1×10⁻⁶ to
190 3.6×10⁻⁵ mol·L⁻¹ (C60 concentration: 6.94×10⁻⁵ mol·L⁻¹). The peak position was also
191 independent of the addition of γ -CDP, however, the peak intensity increased with
192 γ -CDP. Assuming the mole ratio of C60 to CD unit in γ -CDP was 1:2, the formation
193 of the inclusion complex could be calculated as follows:¹¹

$$194 \quad \frac{[H]_0^2[G]_0}{\Delta A} = \frac{[H]_0^2}{\Delta \epsilon} + \frac{K_D}{\Delta \epsilon} \quad (1)$$

195 where H represented the host, CD unit in the polymer, G was the guest, C60, and the
196 initial concentrations of H and G were $[H]_0$ and $[G]_0$ respectively, and $[H]_0 \gg [G]_0$, K_D
197 was the dissociation constant, ΔA was the change in the measured absorbance, and $\Delta \epsilon$
198 was the change in the molar absorption coefficients.

199 Plotting $[H]_0^2[G]_0 / \Delta A$ versus $[H]_0^2$, a straight line was obtained in Fig. 4B.
200 The good linear relationship proved 1:2 ratio of C60 to CD unit in γ -CDP. According
201 to the slope and the intercept of the line, K_D of the inclusion complex was evaluated as
202 $6.36 \times 10^{-5} \text{ mol} \cdot \text{L}^{-1}$. The K_D of C60- γ -CDP was smaller than that of C60- γ -CD
203 ($8.20 \times 10^{-5} \text{ mol} \cdot \text{L}^{-1}$, which was the reciprocal value of the formation constant,
204 $1.22 \times 10^4 \text{ L} \cdot \text{mol}^{-1}$ ³⁹), suggesting that γ -CDP could form the inclusion complex more
205 easily than γ -CD.

206 According to the 1:2 mole ratio of C60 to CD unit in γ -CDP, the water solubility
207 of C60 in C60- γ -CDP was calculated to be $3.0 \times 10^{-4} \text{ mol} \cdot \text{L}^{-1}$. The aqueous solubilities
208 of C60 in different supramolecular inclusion complex^{12, 39-42} are presented in Table 1.
209 It was found that γ -CDP made the aqueous solubility of C60 higher than γ -CD, γ -CD
210 thioether, 6-amino- γ -CD and β -CDP because of its high water solubilities. And it was
211 clear that the solubility of C60 in C60- γ -CDP was about 2×10^8 times greater than that
212 of C60.⁴³ These results revealed that the water-soluble host γ -CDP improved the
213 aqueous solubility of C60 remarkably by the formation of C60- γ -CDP inclusion
214 complex.

215 In short this supramolecular method using γ -CDP had the following three
216 advantages: (i) not only C60 but also other fullerene derivatives with hydrophobic or

217 hydrophilic functional groups could be dispersed; (ii) C60- γ -CDP aqueous solutions
218 with high concentration were stable; and (iii) it could decrease the aggregation of C60,
219 which was good for pharmaceutical applications.

220

221 3.2. Characterization of C60- γ -CDP

222 The number average molecular weight (M_n) of γ -CDP was measured as 55000
223 g·mol⁻¹ by GPC. The typical ¹H NMR spectrum of γ -CDP was presented in the
224 Electronic Supplementary Information (ESI, Fig. S1 (a)), which was consistent with
225 the previous report.³² Although the chemical shift of C60 was not showed in the ¹H
226 NMR spectra of C60- γ -CDP (Fig. S1 (b)), the upfield shifts of CD unit (H1-H6) in
227 C60- γ -CDP distinguished for the ¹H NMR spectra strongly confirmed that C60
228 monomers entered into the hydrophobic CD cavities of γ -CDP, resulting in the change
229 of γ -CDP micro-environment. The result was also similar to our previous studies in
230 CDP inclusion complexes,¹⁰⁻¹² suggested formation of C60- γ -CDP by supramolecular
231 interaction.

232 The inclusion complex was also confirmed by X-ray diffractometry.^{10, 44} Fig. 5
233 shows the X-ray diffraction pattern of (a) C60 and (b) C60- γ -CDP. In Fig. 5 (a), the
234 sharp peaks of C60 at diffraction angles of 2θ 10.8°, 17.7°, 20.8° were observed,
235 showing that C60 existed as a crystalline material. The X-ray diffraction pattern of the
236 C60 inclusion complex in Fig. 5 (b) shows that typical peaks of C60 Peak intensity
237 decreased, a broad peak appeared at $2\theta=18.8^\circ$, and the peaks above 21° disappeared.
238 The complex had a different structure to the parent γ -CDP and C60, indicating that

239 C60- γ -CDP had a new crystalline phase associated with the formation of C60- γ -CDP.
240 The result was in accord with similar observations for the γ -CD complex.³⁷

241 The interaction between γ -CDP and C60 could also be studied from the
242 Raman spectra. The Raman spectrum of γ -CDP was obtained in Fig. 6 (a), and no
243 active Raman was found in the range of the wavenumbers 1200–1800 cm^{-1} . Fig. 6
244 (b) and (c) shows the Raman spectra of C60 and C60- γ -CDP. The Raman dominant
245 peak of C60- γ -CDP at 1470 cm^{-1} represented the stretching mode of cages of C60,
246 which slightly shifted (down to 4 cm^{-1}) compared with that of C60 (1464 cm^{-1})
247 which was similar to C60- β -CDP,¹² and suggested that the formation
248 supramolecular complexes did not change the nature of C60.

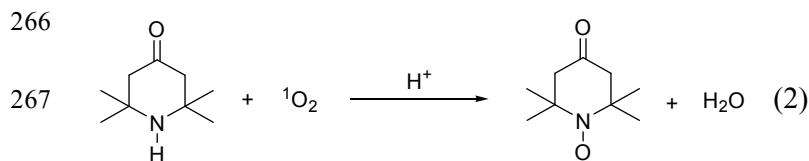
249 The thermal stability of the inclusion complex was determined by TGA in a
250 temperature range of 25-700 °C. Fig. 7 shows the TG curves of the inclusion
251 complexes of (a) C60 and (b) C60- γ -CDP. In Fig. 7 (a) a loss of weight in the 250 °C
252 to 400 °C temperature range corresponding to the thermal decomposition of γ -CDP. In
253 Fig. 7 (b), the mass loss (250-400 °C) corresponding to the decomposition of γ -CDP
254 in the inclusion complex, and C60 was thermally stable. Thus, the amount of C60 was
255 determined to be 18.5 wt% for C60- γ -CDP, and the molar ratio of C60 and γ -CD unit
256 γ -CDP was calculated as 1/1.9 which was close to the above study.

257

258 3.3. Detection of Singlet Oxygen Generation

259 Usually, $^1\text{O}_2$ was detected by the $^1\text{O}_2$ quencher or the direct $^1\text{O}_2$ phosphorescence
260 method. For some researches of C60-CD inclusion complexes,^{34, 35, 45, 46} the $^1\text{O}_2$

261 generation ability of C60-CD was studied by the EPR method. In order to compare the
 262 $^1\text{O}_2$ generation effects between C60- γ -CDP and C60-CD, we chose the EPR method.
 263 It was reported that EPR spectra could study $^1\text{O}_2$ by detecting a nitroxide radical,¹⁸
 264 2,2,6,6-tetramethyl-4-piperidone-N-oxyl radical (TEMPO), which was generated from
 265 TEMP and $^1\text{O}_2$ (2).



268 Fig. S2 in ESI shows the three typical signals of TEMPO, suggesting that TEMP
 269 reacted with $^1\text{O}_2$ to give a $^1\text{O}_2$ adduct, TEMPO, and the relative intensity of the
 270 TEMPO increased with the photoirradiation time. It was meant that C60- γ -CDP
 271 solutions could also produce $^1\text{O}_2$ by UVA photo-irradiation as well as C60/ β -CD and
 272 $(\gamma\text{-CD})_2/\text{C60}$.^{35,46}

273 Fig. 8 shows the EPR intensity of the TEMPO signal as a function of time of
 274 irradiation for C60- γ -CDP solutions with UVA or visible light. The EPR spectra of
 275 C60- γ -CDP showed great rate of $^1\text{O}_2$ production as measured by an increased TEMPO
 276 signal with UVA irradiation. It was reported that C60 aggregation could deactivated
 277 $^1\text{O}_2$ quenching.^{35,47} However, Our result showed that the microenvironment of C60 in
 278 γ -CDP facilitated the generation of $^1\text{O}_2$, because C60 molecules with high
 279 concentration dispersed well in water by formation of γ -CDP inclusion complex.
 280 Therefore, C60- γ -CDP had a high potential for generating $^1\text{O}_2$ with photo-irradiation.
 281 Furthermore, with visible light irradiation, the rate of $^1\text{O}_2$ production was very low
 282 and hardly increased with the irradiation time. The result was different with

283 C60/ β -CD⁴⁶ that C60- γ -CDP could only generate ¹O₂ with UVA irradiation, indicating
284 the possibility of the controllable ¹O₂ production in photodynamic therapy.

285

286 **3.4 The effects of γ -CDP and C60- γ -CDP on cell viability in B16-F10 cells**

287 The biotoxicities of γ -CDP and C60- γ -CDP were very important for the
288 photodynamic therapy. To determine the cytotoxic potential of γ -CDP and C60- γ -CDP,
289 B16-F10 cells were incubated with various concentrations of γ -CDP or C60- γ -CDP
290 for 24 and 48 h and cell viability was evaluated by MTT assay. Fig. 9 A and B show
291 that no cytotoxicity was observed when the C60- γ -CDP complexes were added to the
292 cells in the absence of any exposure to light for 24 and 48 h at concentrations from 0.5
293 μ M to 20 μ M. The similar results showed in Fig. 9 C and D, that γ -CDP did not affect
294 cell viability for 24 and 48 h, indicating γ -CDP could not have a negative impact on
295 the photodynamic therapy and be potential for pharmaceutical carriers. Moreover, the
296 cellular morphological photos of B16-F17 cells were microscopically observed after
297 treatment with C60- γ -CDP or γ -CDP (1-20 μ M) for 48h in ESI. Fig. S3 shows that the
298 density of melanoma cells was almost not reduced by the treatment of C60- γ -CDP,
299 and the morphological photos of the cells with γ -CDP (Fig. S4) were similar to Fig.
300 S3. These result proved that γ -CDP as a host molecule could not only increase the
301 apparent solubility of the guest, but also improve the bioavailability of C60.

302

303 **3.5 Phototoxicity to B16-F10 Cells**

304 For these years, the chemotherapeutic strategies have showed a little effect

305 against metastatic melanoma.⁴⁸ Photodynamic therapy of C60- γ -CDP, as a potential
306 new approach for treatment of dermal melanoma, was studied when the tumor
307 (B16-F10 cells) was irradiated with UVA. To determine the phototoxicity of
308 C60- γ -CDP and C60 on cell viability, B16-F10 cells were initially seeded in
309 microplates followed by different treatments. The results of the MTT assay indicated
310 that no obvious effect on viability was observed when B16-F10 cells were exposed to
311 C60- γ -CDP or C60 in the dark or in the presence of visible light (Fig. 10). With UVA
312 irradiation, however, C60- γ -CDP caused a dramatically reduced rate of cell viability
313 as the increase of C60- γ -CDP. These results were consistent with the above EPR
314 spectra, and they also suggested that $^1\text{O}_2$, which produced by C60- γ -CDP
315 photo-irradiation, induced the efficient damage of B16-F10 cells. Notably, the
316 concentration of C60- γ -CDP which was used to kill B16-F10 cells could be as low as
317 0.5 μM , and the phototoxicity of C60- γ -CDP was about 40 times higher than C60.

318 Because of the high water-soluble γ -CDP and unique electronic π -system of C60,
319 C60- γ -CDP could be dispersed in aqueous solution by formation of CDP inclusion
320 complex and generate $^1\text{O}_2$ upon irradiation with UVA through the energy and electron
321 transfer processes.^{49, 50} The precious results confirmed that C60 inclusion complexes
322 with CD in water were present in C60 aggregation.^{35, 51} As we known, the state of C60
323 aggregation could deactivate the excited electronic states of photo-sensitizers and
324 cause further loss of photo-reactivity, and monomeric C60 were more phototoxic than
325 aggregates of C60.^{34, 35, 50} In this inclusion complex, C60 molecules could penetrate
326 into CD cavities in γ -CDP and prevent to form C60 aggregation. This would explain

327 the observed difference in phototoxicity between C60- γ -CDP and C60, as shown in
328 Fig. 10A.

329 Although C60-CD complexes was not more efficient in photodynamic therapy
330 than C60 derivative²² due to the restriction of CD cavity,³⁹ the supramolecular method
331 by γ -CDP improved C60 water-solubility and biocompatibility practically and
332 provided an easier way to large-scale syntheses of water-soluble fullerene than
333 chemically derivatized method of C60. It was clear that the use of CDP opened
334 opportunities for designing highly versatile inclusion complexes with often improved
335 properties of guest molecules compared to conventional non-CD systems. Because of
336 their fascinating properties, it was expected that CDP based C60 systems would find
337 their way to clinical applications.

338

339 **4. Conclusions**

340 In summary, we developed a simple and fast method to obtain a high
341 water-soluble C60- γ -CDP inclusion complex. The supramolecular interactions
342 between host and guest molecules significantly preserved the integrity of C60, which
343 was critical for many applications. C60- γ -CDP could efficiently generated $^1\text{O}_2$ species
344 with UVA irradiation, and be regarded as a safe inclusion complex due to the low cell
345 toxicity without UVA irradiation. And γ -CDP not only imparted solubility to the
346 hydrophobic C60 in aqueous solution with less aggregation, but also increased
347 biocompatibility efficiently. In addition, C60- γ -CDP with high water solubility and
348 singlet oxygen generation ability showed great phototoxicity for B17-F10 melanoma

349 cells. Furthermore, we believed that the CDP-functionalized methodology would lead
350 to better investigation of the fullerene structure–performance relationship and
351 biomedical applications.

352

353 **Acknowledgements**

354 The authors acknowledged the financial support of the National Natural
355 Science Foundation of China (No. 21273195), the Science and Technology Support
356 Project of Jiangsu Province (No. BE2011738), and the Project Funded by the
357 Priority Academic Program Development of Jiangsu Higher Education Institutions.

358

359 **References**

- 360 1. J. Szejtli, *Chem. Rev.*, 1998, **98**, 1743-1754.
- 361 2. K. A. Connors, *Chem. Rev.*, 1997, **97**, 1325-1358.
- 362 3. W. Zhang, M. Chen and G. Diao, *Carbohydr. Polym.*, 2011, **86**, 1410-1416.
- 363 4. M. Chen, Y. Meng, W. Zhang, J. Zhou, J. Xie and G. Diao, *Electrochim. Acta*,
364 2013, **108**, 1-9.
- 365 5. K. Uekama, F. Hirayama and T. Irie, *Chem. Rev.*, 1998, **98**, 2045-2076.
- 366 6. H. Zou, W. Guo and W. Yuan, *J. Mater. Chem. B*, 2013, **1**, 6235-6244.
- 367 7. D.-S. Guo, K. Wang, Y.-X. Wang and Y. Liu, *J. Am. Chem. Soc.*, 2012, **134**,
368 10244-10250.
- 369 8. W. Zhang, M. Chen, B. Zha and G. Diao, *Phys. Chem. Chem. Phys.*, 2012, **14**,
370 9729-9737.

- 371 9. M. Chen, L. Cui, C. Li and G. Diao, *J. Hazard. Mater.*, 2009, **162**, 23-28.
- 372 10. W. Zhang, M. Chen and G. Diao, *Electrochim. Acta*, 2011, **56**, 5129-5136.
- 373 11. W. Zhang, X. Gong, Y. Cai, C. Zhang, X. Yu, J. Fan and G. Diao, *Carbohydr.*
374 *Polym.*, 2013, **95**, 366-370.
- 375 12. W. Zhang, M. Chen, X. Gong and G. Diao, *Carbon*, 2013, **61**, 154-163.
- 376 13. C. Liu, W. Zhang, Q. Wang, Y. Sun and G. W. Diao, *Org. Biomol. Chem.*, 2013,
377 **11**, 4993-4999.
- 378 14. J. S. Yang and L. Yang, *J. Mater. Chem. B*, 2013, **1**, 909.
- 379 15. F. van de Manakker, T. Vermonden, C. F. van Nostrum and W. E. Hennink,
380 *Biomacromolecules*, 2009, **10**, 3157-3175.
- 381 16. D. M. Guldi and M. Prato, *Acc. Chem. Res.*, 2000, **33**, 695-703.
- 382 17. J. W. Arbogast, A. P. Darmanyan, C. S. Foote, F. N. Diederich, R. L. Whetten,
383 Y. Rubin, M. M. Alvarez and S. J. Anz, *J. Phys. Chem.*, 1991, **95**, 11-12.
- 384 18. Y. Yamakoshi, N. Umezawa, A. Ryu, K. Arakane, N. Miyata, Y. Goda, T.
385 Masumizu and T. Nagano, *J. Am. Chem. Soc.*, 2003, **125**, 12803-12809.
- 386 19. B. Vilenó, A. Sienkiewicz, M. Lekka, A. J. Kulik and L. Forró, *Carbon*, 2004,
387 **42**, 1195-1198.
- 388 20. Y. Choi, Y. Ye, Y. Mackeyev, M. Cho, S. Lee, L. J. Wilson, J. Lee, P. J. J.
389 Alvarez, W. Choi and J. Lee, *Carbon*, 2014, **69**, 92-100.
- 390 21. S. Bosi, T. Da Ros, G. Spalluto and M. Prato, *Eur. J. Med. Chem.*, 2003, **38**,
391 913-923.
- 392 22. L. Huang, M. Terakawa, T. Zhiyentayev, Y. Y. Huang, Y. Sawayama, A. Jahnke,

- 393 G. P. Tegos, T. Wharton and M. R. Hamblin, *Nanomedicine: NBM*, 2010, **6**,
394 442-452.
- 395 23. G. P. Tegos, T. N. Demidova, D. Arcila-Lopez, H. Lee, T. Wharton, H. Gali
396 and M. R. Hamblin, *Chem. Biol.*, 2005, **12**, 1127-1135.
- 397 24. G. L. Marcorin, T. Da Ros, S. Castellano, G. Stefancich, I. Bonin, S. Miertus
398 and M. Prato, *Org. Lett.*, 2000, **2**, 3955-3958.
- 399 25. Q. Zhang, Z. Jia, S. Liu, G. Zhang, Z. Xiao, D. Yang, L. Gan, Z. Wang and Y.
400 Li, *Org. Lett.*, 2009, **11**, 2772-2774.
- 401 26. S. Aroua, W. B. Schweizer and Y. Yamakoshi, *Org. Lett.*, 2014, **16**, 1688-1691.
- 402 27. T. Hamano, K. Okuda, T. Mashino, M. Hirobe, K. Arakane, A. Ryu, S.
403 Mashiko and T. Nagano, *Chem. Commun.*, 1997, 21-22.
- 404 28. F. Prat, R. Stackow, R. Bernstein, W. Qian, Y. Rubin and C. S. Foote, *J. Phys.*
405 *Chem. A*, 1999, **103**, 7230-7235.
- 406 29. A. Ikeda, *J. Incl. Phenom. Macrocycl. Chem.*, 2013, **77**, 49-65.
- 407 30. Y. Chen and Y. Liu, *Chem. Soc. rev.*, 2010, **39**, 495-505.
- 408 31. E. L. Clennan and A. Pace, *Tetrahedron*, 2005, **61**, 6665-6691.
- 409 32. V. Wintgens and C. Amiel, *Eur. Polym. J.*, 2010, **46**, 1915-1922.
- 410 33. E. Renard, A. Deratani, G. Volet and B. Sebille, *Eur. Polym. J.*, 1997, **33**,
411 49-57.
- 412 34. B. Zhao, Y.-Y. He, P. J. Bilski and C. F. Chignell, *Chem. Res. Toxicol.*, 2008,
413 **21**, 1056-1063.
- 414 35. B. Zhao, Y.-Y. He, C. F. Chignell, J.-J. Yin, U. Andley and J. E. Roberts, *Chem.*

- 415 *Res. Toxicol.*, 2009, **22**, 660-667.
- 416 36. C. N. Murthy and K. E. Geckeler, *Chem. Commun.*, 2001, 1194-1195.
- 417 37. D.-D. Zhang, Q. Liang, J.-W. Chen, M.-K. Li and S.-H. Wu, *Supramol. Chem.*,
- 418 1994, **3**, 235-239.
- 419 38. K. Fujita, S. Ejima and T. Imoto, *Chem. Lett.*, 1985, **14**, 11-12.
- 420 39. K. I. Priyadarsini, H. Mohan, A. K. Tyagi and J. P. Mittal, *J. Phys. Chem.*,
- 421 1994, **98**, 4756-4759.
- 422 40. H. M. Wang and G. Wenz, *Beilstein J. Org. Chem.*, 2012, **8**, 1644-1651.
- 423 41. K. Nobusawa, M. Akiyama, A. Ikeda and M. Naito, *J. Mater. Chem.*, 2012, **22**,
- 424 22610.
- 425 42. S. Deguchi, R. G. Alargova and K. Tsujii, *Langmuir*, 2001, **17**, 6013-6017.
- 426 43. J. D. Fortner, D. Y. Lyon, C. M. Sayes, A. M. Boyd, J. C. Falkner, E. M. Hotze,
- 427 L. B. Alemany, Y. J. Tao, W. Guo, K. D. Ausman, V. L. Colvin and J. B.
- 428 Hughes, *Environ. Sci. Technol.*, 2005, **39**, 4307-4316.
- 429 44. H.-C. Hu, Y. Liu, D.-D. Zhang and L.-F. Wang, *J. Incl. Phenom. Macro.*, 1999,
- 430 **33**, 295-305.
- 431 45. Y. Liu, P. Liang, Y. Chen, Y.-L. Zhao, F. Ding and A. Yu, *J. Phys. Chem. B*,
- 432 2005, **109**, 23739-23744.
- 433 46. D. Iohara, M. Hiratsuka, F. Hirayama, K. Takeshita, K. Motoyama, H. Arima
- 434 and K. Uekama, *J. Pharm. Sci.*, 2012, **101**, 3390-3397.
- 435 47. P. Bilski, B. Zhao and C. F. Chignell, *Chem. Phys. Lett.*, 2008, **458**, 157-160.
- 436 48. B. Zhao, J. J. Yin, P. J. Bilski, C. F. Chignell, J. E. Roberts and Y. Y. He,

- 437 *Toxicol. Appl. Pharmacol.*, 2009, **241**, 163-172.
- 438 49. B. Zhao, P. J. Bilski, Y.-Y. He, L. Feng and C. F. Chignell, *Photochem.*
439 *Photobiol.*, 2008, **84**, 1215-1223.
- 440 50. A. R. Wielgus, B. Zhao, C. F. Chignell, D.-N. Hu and J. E. Roberts, *Toxicol.*
441 *Appl. Pharmacol.*, 2010, **242**, 79-90.
- 442 51. D. Iohara, F. Hirayama, K. Higashi, K. Yamamoto and K. Uekama, *Mol.*
443 *pharmaceutics*, 2011, **8**, 1276-1284.
- 444
- 445

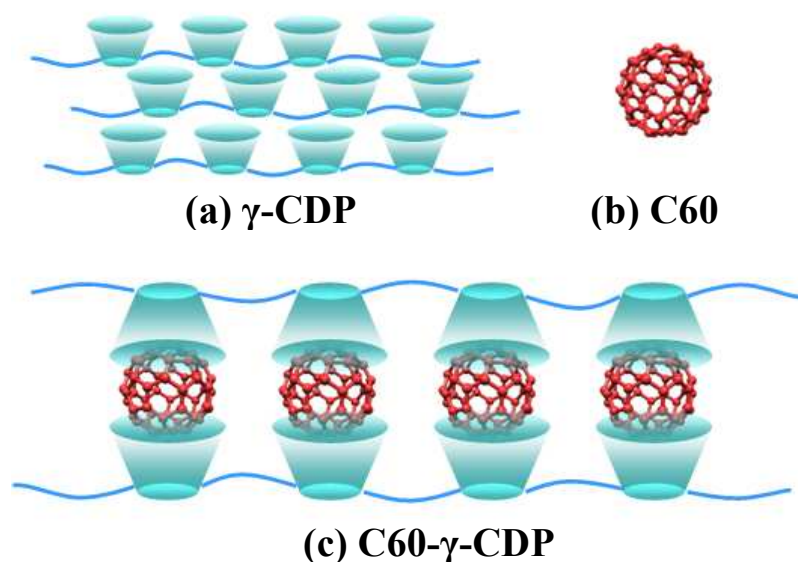
446 **Table 1** Aqueous solubility of C60 in different supramolecular inclusion complex

Sample	Concentration of C60 in aqueous solubility (mol·L ⁻¹)	Reference
C60- γ -CDP	3.0×10^{-4}	our work
C60/ γ -CD	1.0×10^{-4}	39
C60/ γ -CD thioether	2.1×10^{-5}	40
C60/6-amino- γ -CD	1.0×10^{-5}	41
C60- β -CDP	6.7×10^{-5}	12
C60 cluster	1.0×10^{-5}	42
C60	$<1.4 \times 10^{-12}$	43

447

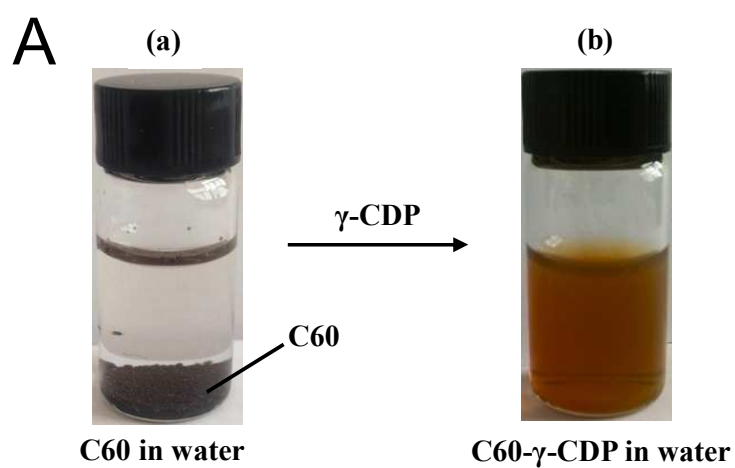
448

449

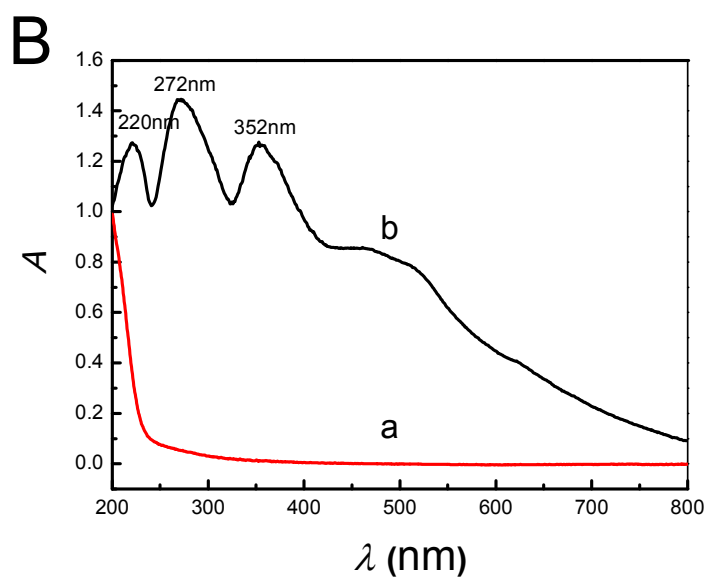


450
451
452

Fig. 1 Schematic illustration of (a) γ -CDP, (b) C60, and (c) C60- γ -CDP



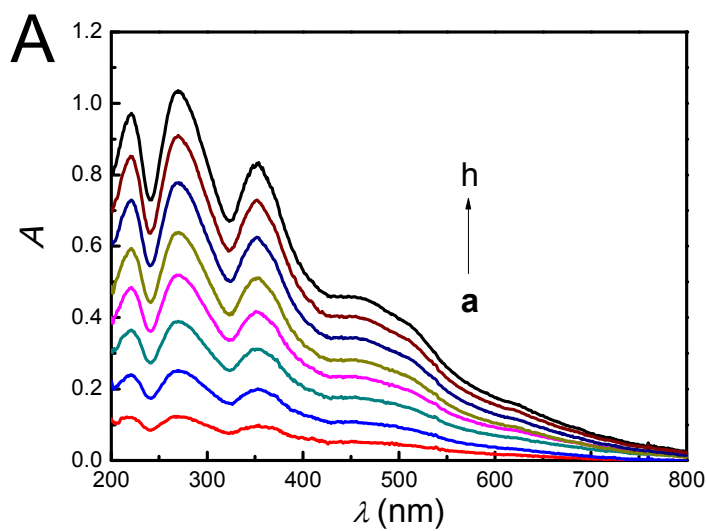
453



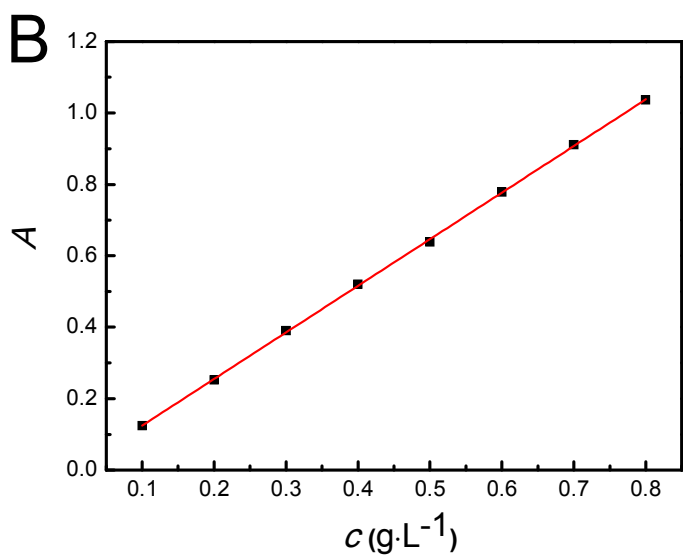
454

455 **Fig. 2A** Photographs of (a) C60 and (b) C60- γ -CDP in water. **B** UV spectra of (a) C60456 and (b) C60- γ -CDP in aqueous solution pH=7.0, at 25°C.

457

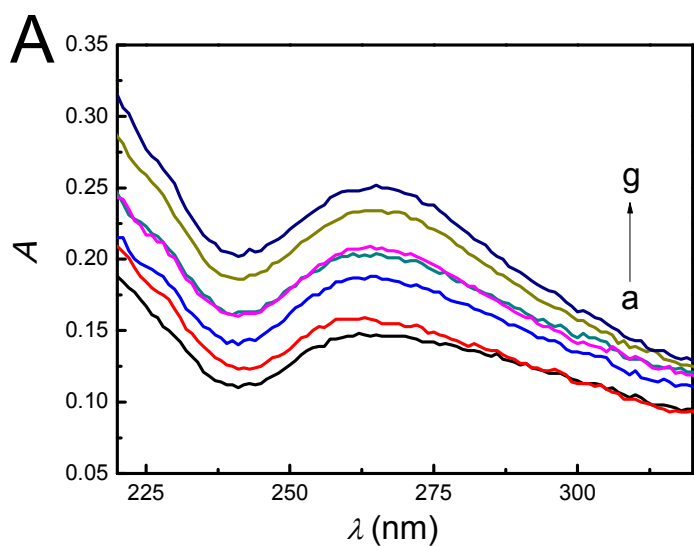


458

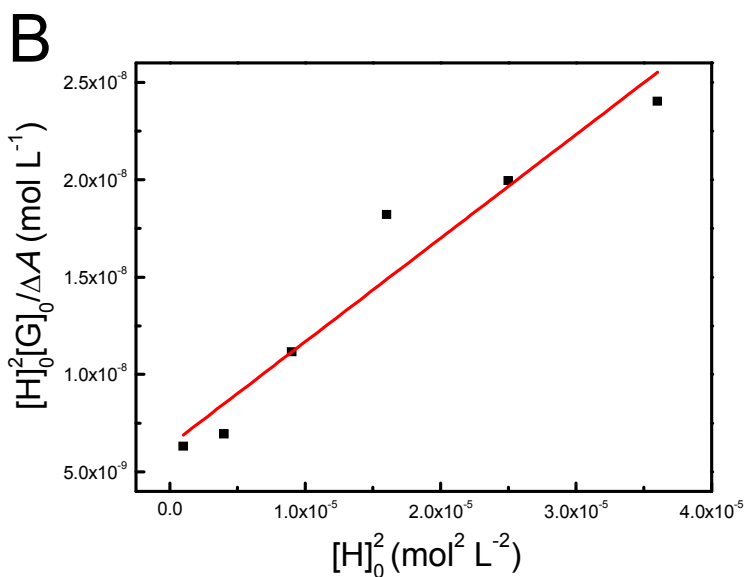


459

460 **Fig. 3A** UV spectra of C60- γ -CDP with different concentrations (g L^{-1}) in aqueous
461 solution (pH=7.0, 25 $^{\circ}\text{C}$): (a) 0.1, (b) 0.2, (c) 0.3, (d) 0.4, (e) 0.5, (f) 0.6, (g) 0.7, and (h)
462 0.8. **B** A plot of absorbance ratio of C60- γ -CDP at 272 nm vs. the concentration of
463 C60- γ -CDP, Data taken from **Fig. 3A**.



464



465

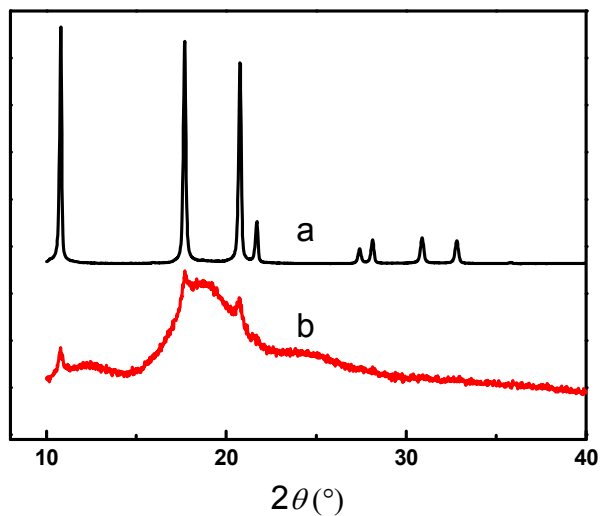
466 **Fig. 4A** At 25 °C, UV spectra of $6.94 \times 10^{-5} \text{ mol} \cdot \text{L}^{-1}$ C60 in ethylene glycol with

467 different concentrations of γ -CD unit in CDP ($\text{mol} \cdot \text{L}^{-1}$): (a) 0, (b) 1×10^{-6} , (c) 4×10^{-6} , (d)

468 9×10^{-6} , (e) 1.6×10^{-5} , (f) 2.5×10^{-5} , (g) 3.6×10^{-5} . **B** The plot of $[\text{H}]_0^2[\text{G}]_0 / \Delta A$ vs. $[\text{H}]_0^2$.

469 Data taken from **Fig. 4A**.

470

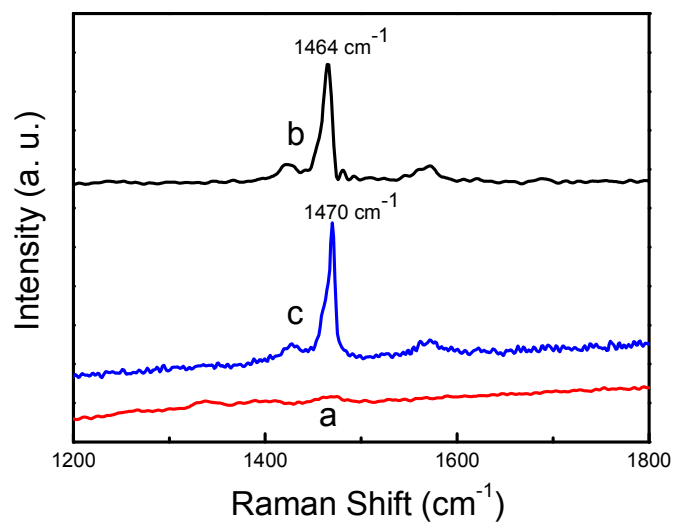


471

472 **Fig. 5** Powder X-ray diffraction patterns of (a) C60 and (b) C60-γ-CDP.

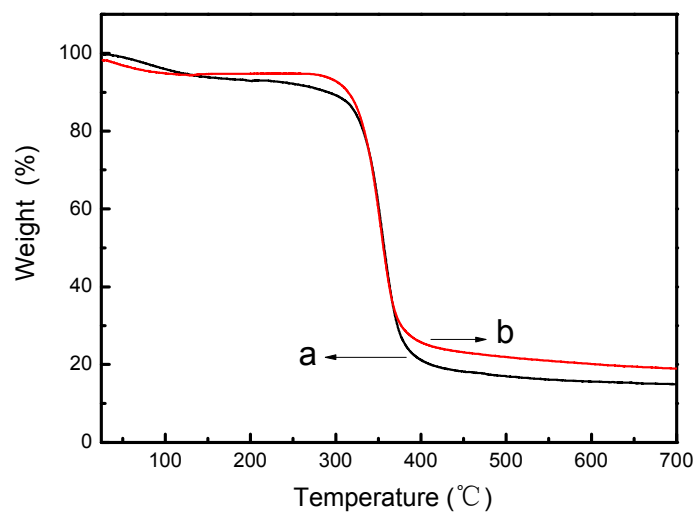
473

474



475

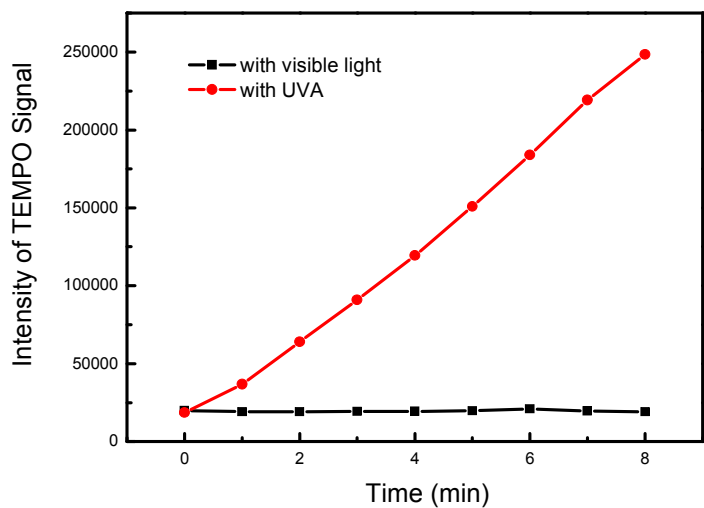
476 **Fig.6** Raman spectra of (a) γ-CDP, (b) C60, and (c) C60-γ-CDP.



477

478 **Fig. 7** TG curves of (a) γ -CDP and (b) C60- γ -CDP.

479

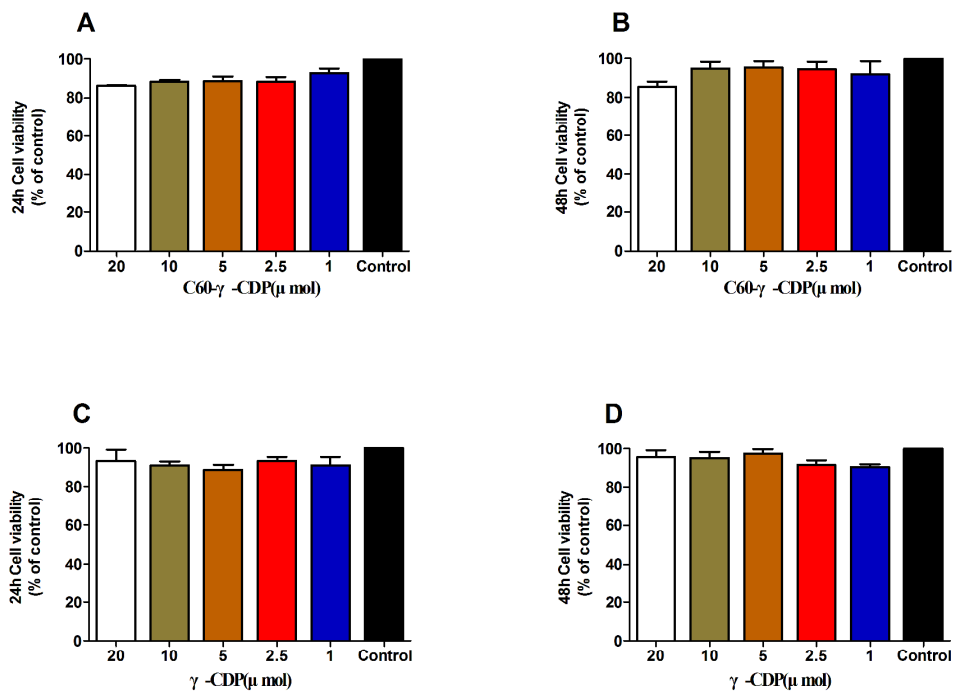


480

481 **Fig.8** Intensity of TEMPO signals as a function of time during UVA or visible light482 irradiation of C60- γ -CDP water solution.

483

484



485

486 **Fig. 9** *In vitro* cytotoxicity of 1-20 μ M C60- γ -CDP (A 24h and B 48h) and γ -CDP (C
487 24h and D 48h) following the MTT assay.

488

489

490

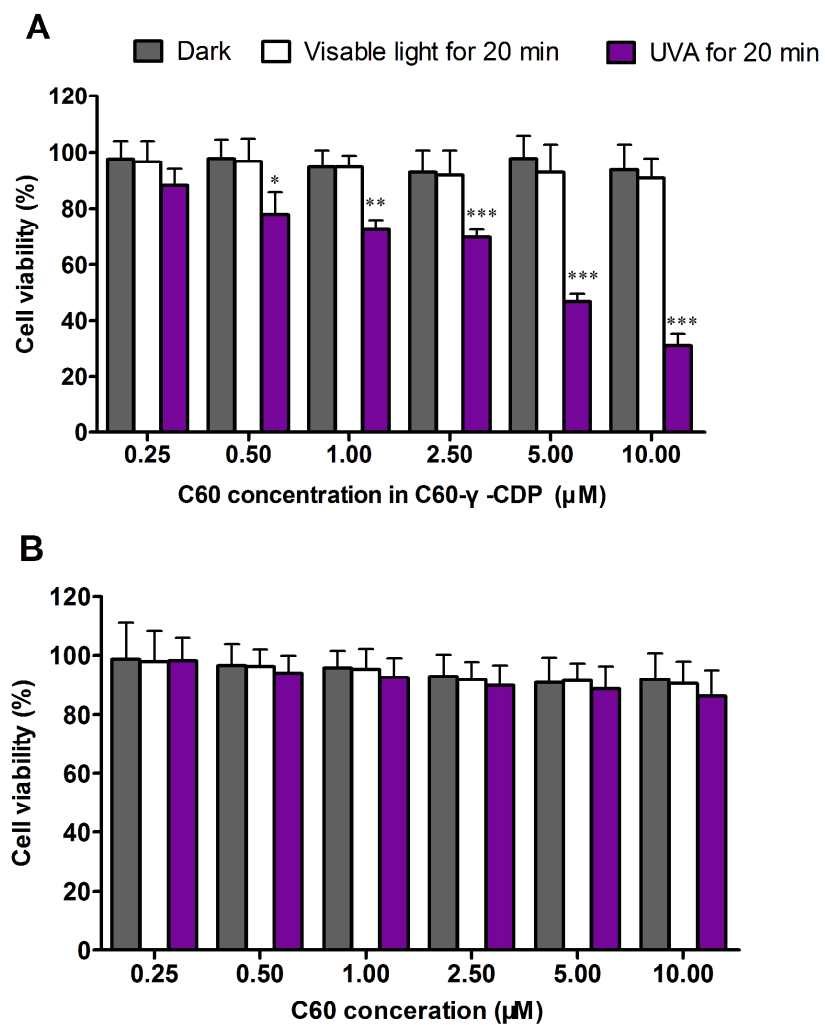
491

492

493

494

495



496

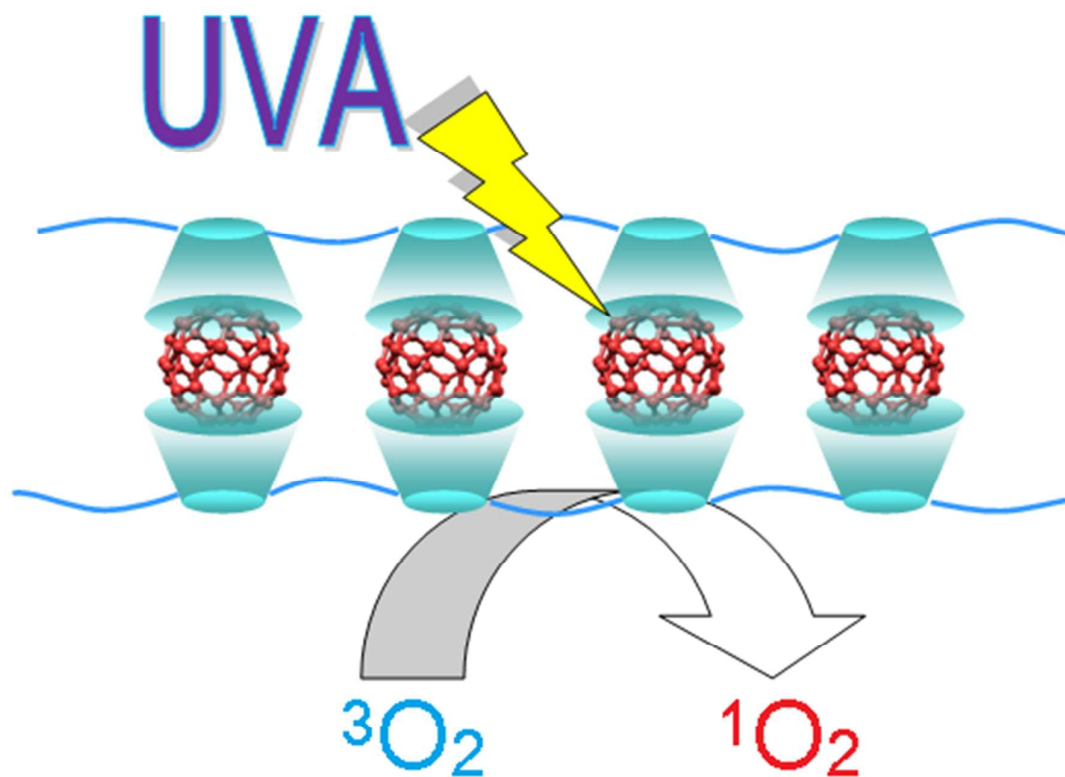
497 **Fig. 10** Effect of different concentrations of (A) C60- γ -CDP and (B) C60 exposure on
498 the viability of B16-F10 cells irradiated with UVA and cool white light as measured
499 by the MTT assay (see the Materials and Methods).

500

501

502

A table of contents entry



Text:

A method was developed to obtain a high water-soluble C₆₀- γ -CDP inclusion complex, which could efficiently generate $^1\text{O}_2$ species with UVA irradiation.